Electronic Supplementary Information for Dalton Transactions

Spectroscopic, Electrochemical and Computational Study of Pt-diimine-dithiolene Complexes in the Context of Solar Cell Dyes

Elaine A. M. Geary,[a] Keri L. McCall,[a] Andrew Turner,[a] Eric J. L. McInnes,[b] Lesley J. Yellowlees,[a] and Neil Robertson*[a]

Electronic.Supplementary Information

UV/Vis/NIR spectroelectrochemistry (OTTLE)

UV/Vis/NIR spectroelectrochemistry was performed to electronically characterise the frontier orbitals of compounds **1c, 2c** and **3c**. This involved electrochemical reduction of **1c, 2c** and **3c** to $\mathbf{1c^{1-}}$, $\mathbf{2c^{1-}}$ and $\mathbf{3c^{1-}}$ and also to $\mathbf{1c^{2-}}$, $\mathbf{2c^{2-}}$ and $\mathbf{3c^{2-}}$ respectively. On comparison of each species to its related platinum dichloro precursor and uncoordinated free ligand in their related neutral, monoreduced and direduced states, attempts can be made to assign the location of the reduction electron in the monoreduced and direduced complexes. For this purpose a detailed analysis of **2a**, **2b** and **2c** is given, however this same analysis applies within **1a-1c** and **3a-3c**, as each series behaves in a similar fashion. Peaks observed and their relative molar extinction coefficient (ε) values are shown in table S1.

Table S1 Peaks observed in the UV/visible spectra for complexes in their monooxidised (**+1**), neutral (**0**), monoreduced (**-1**) and direduced (**-2**) states. ε /$M^{-1}cm^{-1}$ are given in brackets.

Complex	+1, **ν/cm^{-1}** (**ε /$M^{-1}cm^{-1}$**)	0, **ν/cm^{-1}** (**ε /$M^{-1}cm^{-1}$**)	-1, **ν/cm^{-1}** (**ε /$M^{-1}cm^{-1}$**)	-2, **ν/cm^{-1}** (**ε /$M^{-1}cm^{-1}$**)
1a	**----**	**37,200 (6,600)**	**37,200 (8,300)**	**---------**
			25,300 (2,500)	
1b	**----**	**33,900 (14,700)**	**33,200 (15,400)**	**32,400 (21,200)**
		29,800 (5,100)	**24,400 (9,800)**	**27,000 (13,300)**
		26,900 (1,700)	**22,100 (7,200)**	**10,800 (3,300)**
		23,200 (2,700)	**20,400 (5,800)**	
1c	**31,600 (16,900)**	**32,000 (25,600)**	**30,000 (21,350)**	**33,500 (23,400)**
	23,000 (3,800)	**25,700 (5,900)**	**25,300 (10,600)**	**27,400 (23,200)**

	18,300 (2,900)	**18,300 (6,300)**	**22,900 (12,400)**	**23,600 (6,900)**
			19,400 (9,000)	**20,600 (1,500)**
				19,300 (1,000)
2a	**--------**	**33,200 (14,000)**	**33,100 (15,400)**	**----------**
		32,000 (10,800)	**26,700 (6,800)**	
			25,000 (9,200)	
			18,000 (5,500)	
			16,400 (3,500)	
			11,150 (1,300)	
2b	**---------**	**33,700 (22,350)**	**32,200 (19,900)**	**36,400 (15,800)**
		30,300 (9,000)	**26,300 (11,800)**	**32,900 (19,800)**
		29,000 (8,800)	**22,200 (4,500)**	**31,500 (19,600)**
		25,700 (2,600)	**21,200 (4,300)**	**27,600 (20,500)**
		24,300 (4,400)	**19,700 (4,900)**	**24,300 (10,300)**
			15,900 (600)	**19,700 (3,500)**
			8,700 (2,600)	**10,600 (11,600)**
			7,100 (6,500)	
2c	**29,800 (16,900)**	**34,200 (16,300)**	**33,100 (17,900)**	**33,300 (22,900)**
	22,200 (5,000)	**31,400 (21,000)**	**31,500 (18,100)**	**27,300 (28,600)**
	18,300 (2,500)	**27,500 (6,600)**	**29,200 (19,100)**	**24,200 (16,200)**
		18,900 (6,300)	**27,000 (15,400)**	**10,300 (7,400)**
			21,200 (7,200)	
			19,600 (7,500)	
			18,200 (5,300)	
			15,900 (3,600)	
			8,300 (2,700)	
			7,000 (4,700)	
3a	**----**	**32,900 (26,600)**	**33,100 (16,000)**	**33,500 (10,400)**
			24,700 (2,700)	**23,100 (4,300)**
			24,000 (4,900)	**22,800 (5,800)**
			22,900 (6,100)	**22,200 (7,800)**
			22,200 (9,900)	**20,600 (6,600)**
			21,000 (3,000)	**19,000 (5,800)**
			19,800 (2,700)	
			14,400 (2,600)	
			13,000 (4,000)	
			12,300(2,600)	
			11,000 (800)	
3b	**----**	**37,600 (18,900)**	**33,700 (12,600)**	**32600 (11,500)**
		33,800 (24,000)	**31,900(12,200)**	**25,100 (6,300)**
		30,500 (12,300)	**29,700 (9,300)**	**23,600 (11,400)**
		29,400 (14,200)	**26,600 (7,100)**	**22,200 (29,000)**
		24,800 (2,800)	**24,900 (11,900)**	**20,800 (49,300)**
		23,800 (3,200)	**22,000 (4,200)**	

			20,500 (5,000)	
			18,800 (4,200)	
			16,200 (6,900)	
3c	**30,400 (12,100)**	**33,900 (14,100)**	**34,300 (15,600)**	**36,000 (14,400)**
	23,200 (2,700)	**31,800 (11,400)**	**31,500 (13,200)**	**28,400 (9,600)**
	18,400 (2,200)	**30,000 (12,300)**	**30,000 (12,300)**	**23,700 (11,700)**
		25,700 (1,900)	**25,700 (7,100)**	**22,300 (25,500)**
		18,400 (2,000)	**22,000 (5,300)**	**20,700 (55,500)**
			16,900 (3,700)	**17,800 (4,400)**
				16,300 (2,500)

The spectrum of the neutral ligand **2a** shows one intense band at greater than 30,000 cm^{-1} which is assigned as a π-π^* intraligand bpy transition. Reduction of the neutral molecule to give $\mathbf{2a^{1-}}$ results in the formation of three new bands at *ca.* 12,000 cm^{-1}, *ca.* 18,000 cm^{-1} and *ca.* 25,000 cm^{-1}. These are assigned as π-π* transitions of the monoreduced disubstituted bpy ligand. The spectrum of bpy^{1-} has previously been studied and three sets of absorption bands that are diagnostic for the presence of co-ordinated bpy^{1-} have been assigned (E. Koenig and S. Kremer, *Chem. Phys. Lett.*, 1970, **5**, 87). These are i) a NIR band at *ca.* 10,000 cm^{-1}, ii) a visible band at *ca.* 20,000 cm^{-1} and iii) an intense near UV band at *ca.* 25,000 cm^{-1}. Therefore the spectrum of $\mathbf{2a^{1-}}$ is similar to that of bpy^{1-}. It is not possible to record the spectrum of the direduced species ($\mathbf{2a^{2-}}$) since the reduction potential occurs outside of the solvent window.

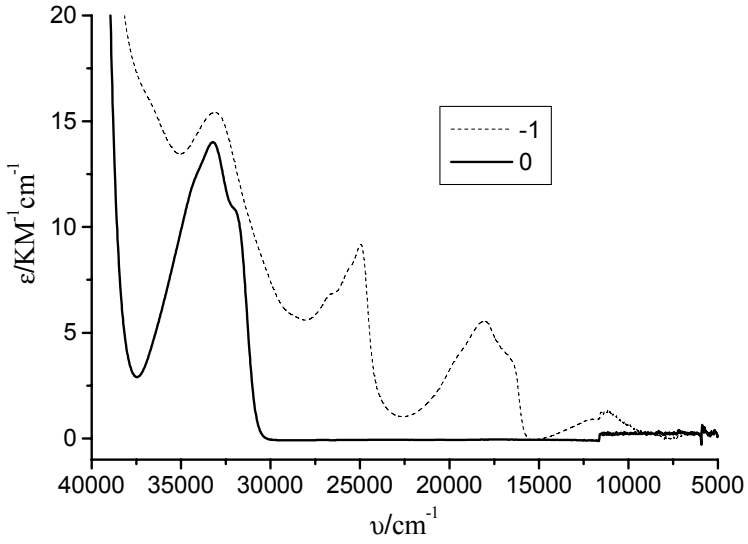

Fig. S1 UV/visible spectra of $\mathbf{2a}^{0/1-}$ in 0.1 M solution of $TBABF_4$ in DMF at 213 K. E_{gen} = 0 V(0), -1.86 V(-1)

The spectrum of the neutral dichloro complex **2b** shows a π-π^* transition at greater than 30,000 cm^{-1} as seen in the spectrum of **2a**. In addition to this, a peak at 25,000 cm^{-1} is assigned as the MLCT of the Pt-bpy transition. On reduction of this species to $\mathbf{2b}^{1-}$ the peak representing the π-π^* transition of the neutral species decreases, there is a growth of a peak at *ca.* 27,000 cm^{-1} as well as a band at *ca.* 20,000 – 22,000 cm^{-1}, a band at at *ca.* 16,000 cm^{-1} and a peak in the NIR. This spectrum is similar to that of $\mathbf{2a}^{1-}$ and therefore implies that the reduction electron in the monoreduced complex locates itself on the derivatised bpy ligand. The direduced species $\mathbf{2b}^{2-}$ shows a broadening of the peak above 30,000 cm^{-1} with a shoulder at *ca*. 24,000 cm^{-1}, growth of the peak at *ca.* 28,000 cm^{-1} and an intense peak in the NIR.

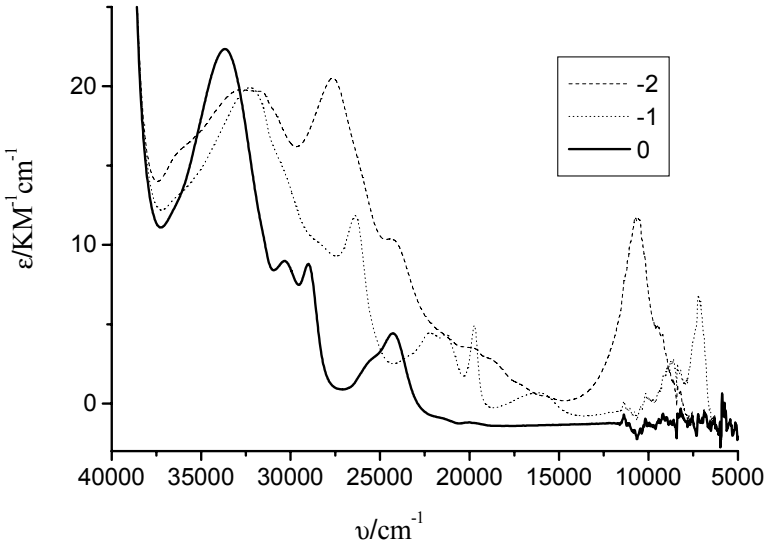

Fig. S2 UV/visible spectra of $\mathbf{2b}^{0/1-/2-}$ in 0.1 M solution of $TBABF_4$ in DMF at 213 K. E_{gen} = 0 V(0), -1.1 V(-1) and -1.81 V(-2)

The spectrum of the neutral mnt complex **2c** shows a peak at greater than 30,000 cm^{-1} assigned as the π-π^* intraligand transition of the derivatised bpy motif. The shoulder at *ca.* 30,000 – 25,000 cm^{-1} is assigned as the MLCT previously seen in **2b** however the intensity of this peak may be slightly masked by a new peak at *ca.* 20,000 cm^{-1} which is assigned as a MMLL′CT from the Pt/mnt to bpy. Reduction of this species to $\mathbf{2c}^{1-}$ results in a spectrum with a broad band at greater than 30,000 cm^{-1}, a shoulder at *ca.* 28,000 cm^{-1}, a broad band from *ca.* 17,500 – 22,000 cm^{-1}, a band at *ca*. 16,000 cm^{-1} and a peak in the NIR. This spectrum is very similar to that of $\mathbf{2b}^{1-}$, implying that in both cases the reduction electron locates itself in the same place i.e. the derivatised bpy ligand. The direduced species $\mathbf{2c}^{2-}$ shows a peak above 30,000 cm^{-1}, growth of the peak at *ca.* 27,000 cm^{-1} with a shoulder at 24,000 cm^{-1} and an intense peak in the NIR, which is again similar to that of $\mathbf{2b}^{2-}$ showing that the second reduction electron in $\mathbf{2c}^{2-}$ is located in the same place as it is in $\mathbf{2b}^{2-}$. The UV/Vis/NIR spectroelectrochemistry suggests that in each case, the reduction electron enters an orbital which is primarily located on the bpy. This is consistent with previous reports of a bpy based LUMO and supplements the findings of the electrochemical study. Note that the band associated with the MMLL′CT

no longer features in the UV/visible spectrum of $\mathbf{2c}^{2-}$ since the LUMO which is located on the bpy is now fully occupied.

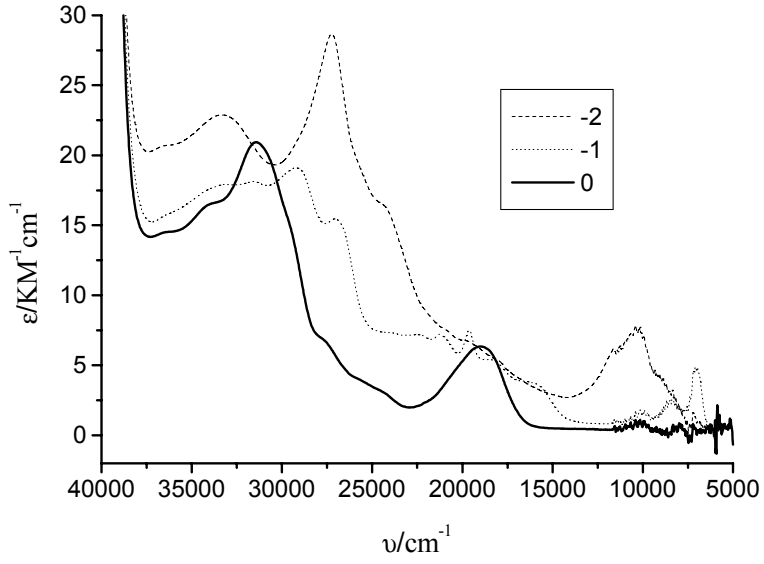

Fig. S3 UV/visible spectra of $\mathbf{2c}^{0/1-/2-}$ in 0.1 M $TBABF_4$/DMF at 213 K. E_{gen}= 0 V(0), -1.0 V(-1), -1.6 V(-2)

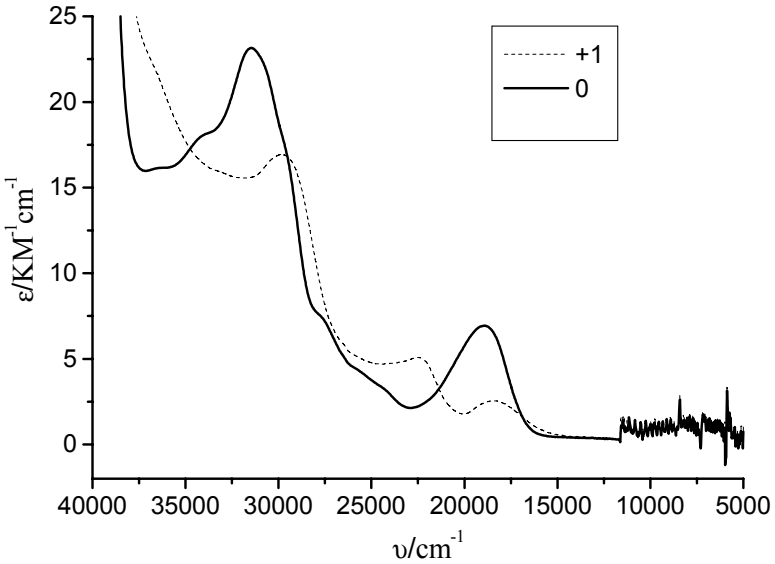

Fig. S4 UV/visible spectra of $\mathbf{2c}^{0/1+}$ in 0.1 M $TBABF_4$/DMF at 213 K. E_{gen}= 0 V(0), 1.5 V(+1).

For each ligand and complex, in every case after recording the final spectrum the potential was adjusted so that the neutral starting material was regenerated and each absorption spectrum was observed to return to exactly that of the starting species. Thus the monooxidised, monoreduced and direduced species of [Pt{X,X′(CO_2Et)$_2$-bpy}(mnt)] and its precursor molecules are all stable at 213 K.

In-situ EPR Spectroelectrochemistry

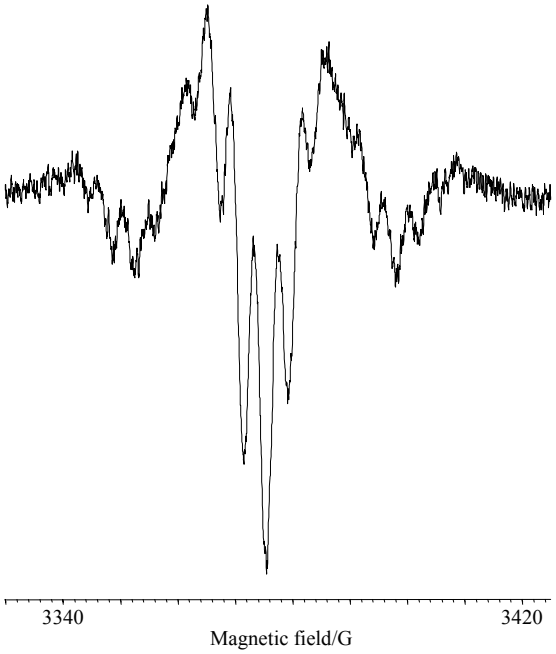

Fig. S5 EPR spectrum of $\mathbf{1b}^{1-}$ in 0.1 M $TBABF_4$/DMF at 293 K

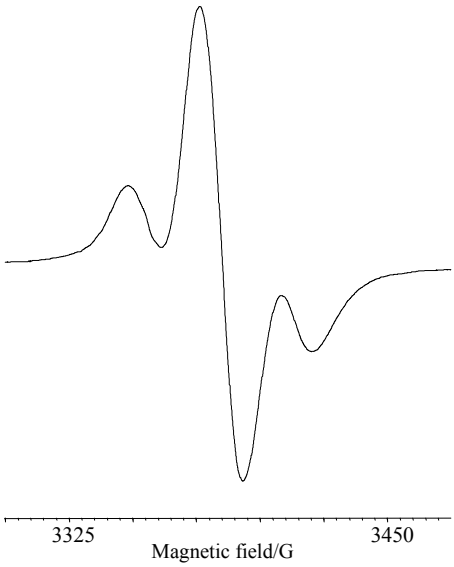

Fig. S6 EPR spectrum of $\mathbf{2c}^{1-}$ in solution of 0.1 M $TBABF_4$ in DMF at 293 K. E_{gen} = -1.15 V

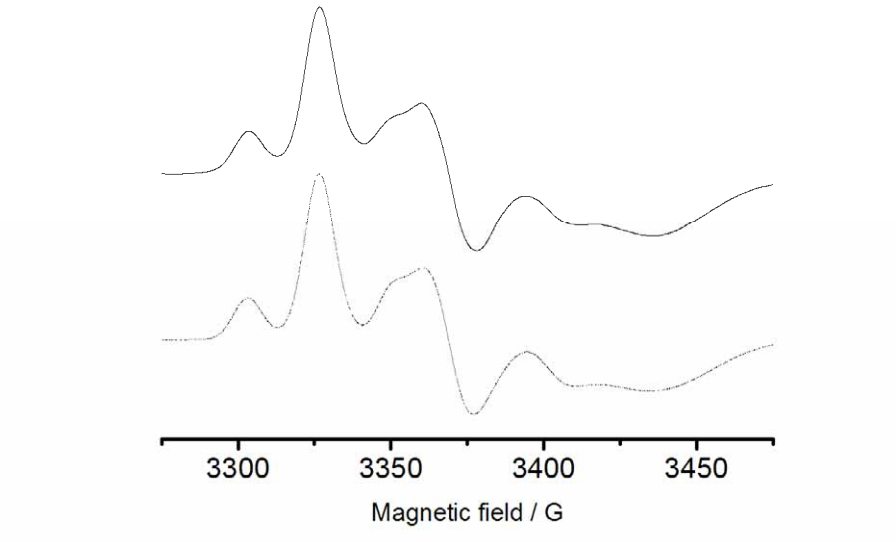

Fig. S7 EPR spectrum of $\mathbf{1b}^{1-}$ in solution of 0.1 M $TBABF_4$ in DMF at 173 K. Simulated spectrum also shown.

DFT Calculations on Ligands

Calculated gas-phase structure of trans 4,4' ligand (2a)

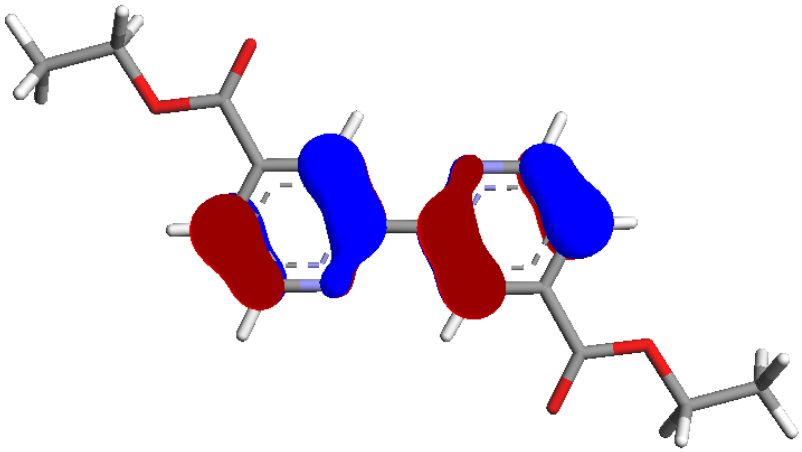

Fig. S8: Calculated HOMO of trans 4,4' ligand (**2a**)

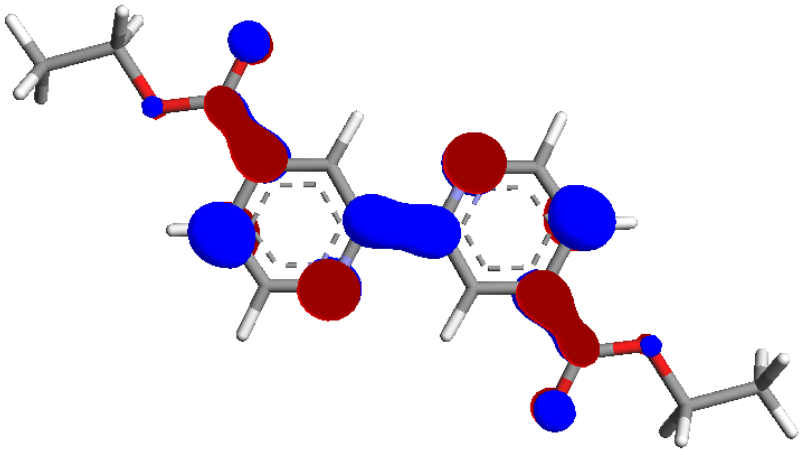

Fig. S9: Calculated LUMO of trans 4,4' ligand (**2a**)

Orbital	Hartrees	eV	cm-1
HOMO	-0.24652	-6.70815	54104.61
LUMO	-0.0724	-1.97011	15889.88
HOMO-1	-0.2585	-7.03415	56733.9
LUMO+1	-0.0647	-1.76058	14199.94

Table S2: Orbital energies of **2a**

Calculated gas-phase structure of trans 5,5' ligand (3a)

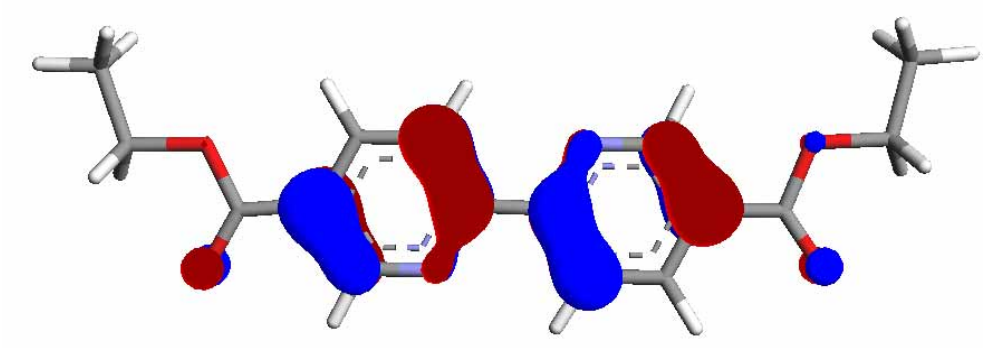

Fig. S10: Calculated HOMO of **3a**

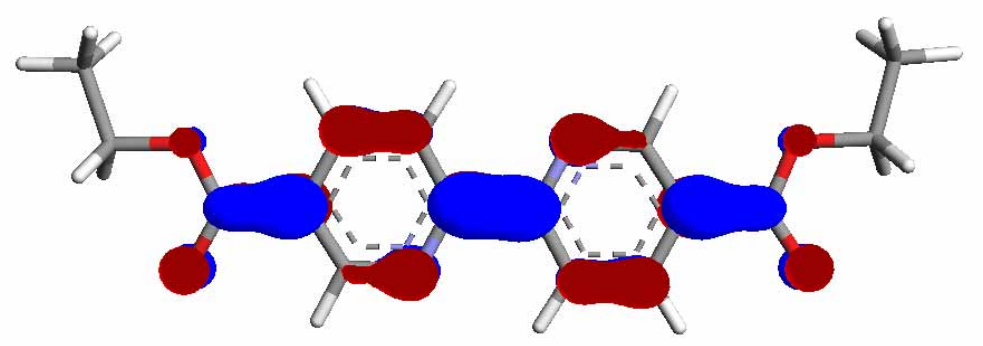

Fig. S11: Calculated LUMO of **3a**

Orbital	Hartrees	eV	cm-1
HOMO	-0.25172	-6.84965	55245.87
LUMO	-0.08675	-2.36059	19039.33
HOMO-1	-0.26019	-7.08013	57104.81
LUMO+1	-0.03825	-1.04084	8394.862

Table S3: Orbital energies of **3a**

DFT Calculations on Complexes

	N	C (3-position)	C (4-position)	C (5-postion)	C (6-position)
1c	**0.093**	**-**	**0.025**	**0.097**	**0.002**
2c	**0.132**	**0.006**	**-**	**0.090**	**0.093**
3c	**0.086**	**0.037**	**0.053**	**-**	**0.003**

Table S4: Calculated contribution to the LUMO of the neutral complexes [Pt{X,X′-$(CO_2Et)_2$-bpy}(mnt)] from the bipy-ring N and C atoms that have hydrogen substituents.

Complex	HOMO / eV	LUMO / eV	HOMO-1 / eV	LUMO+1 / eV
1b	-5.271801	-3.989905	-5.544724	-3.131407
1c	-5.54187	-3.68551	-6.65482	-2.75624
2c	-5.58922	-3.70973	-6.7038	-2.97448
3c	-5.4801	-3.75272	-6.58978	-2.4844

Table S5:Calculated energies of HOMO, LUMO, HOMO-1 and LUMO+1 of **1b, 1c**, **2c** and **3c**

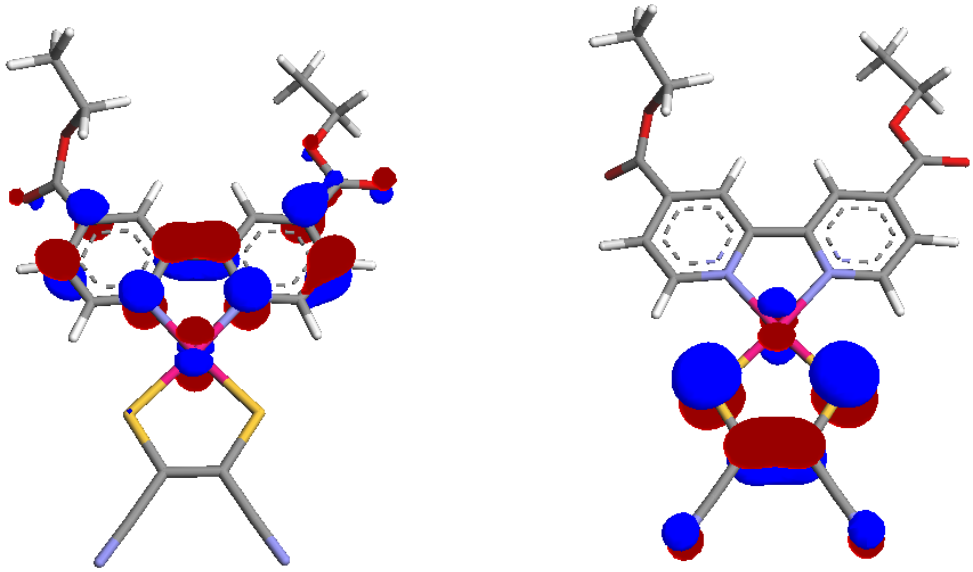

Fig. S12 Calculated LUMO (left) and HOMO (right) of **2c**

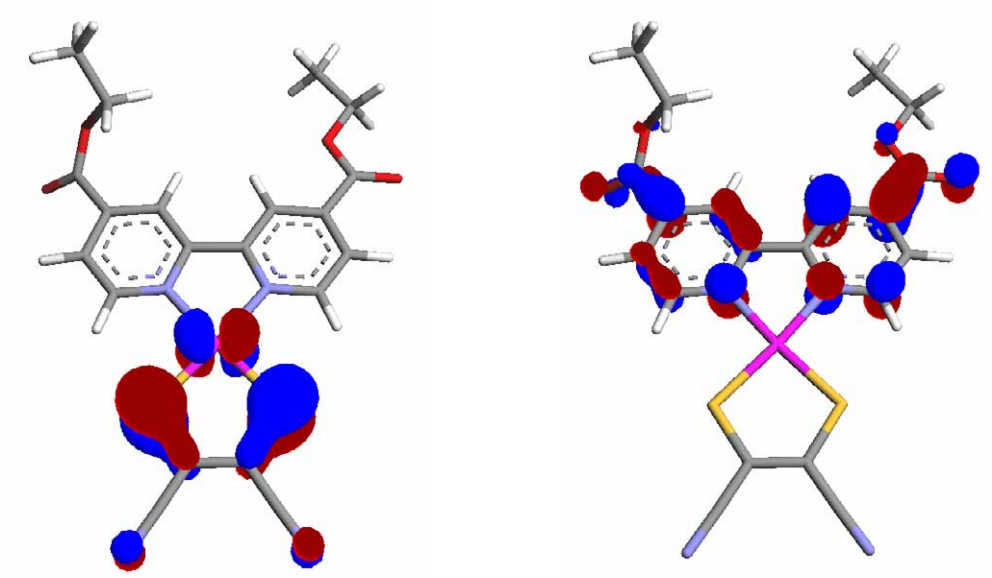

Fig. S13 Calculated HOMO-1 (left) and LUMO+1 (right) of **2c**

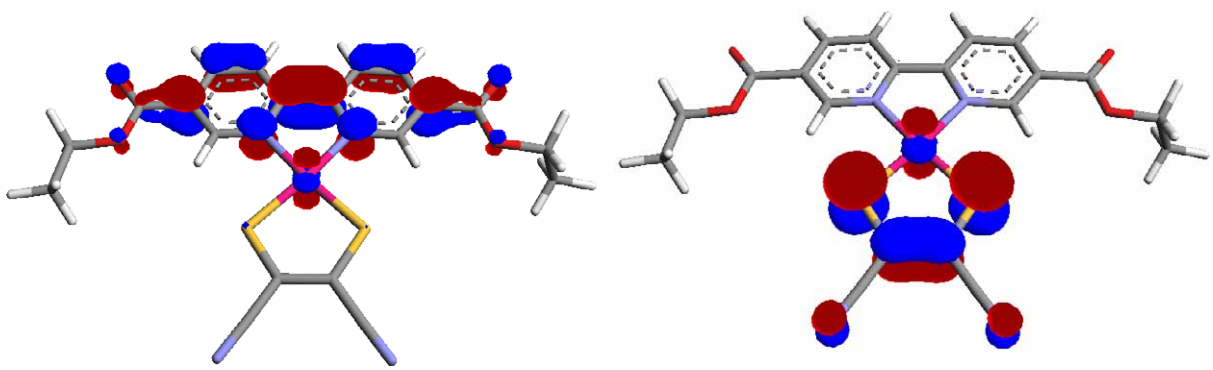

Fig. S14 Calculated LUMO (left) and HOMO of **3c** (right)

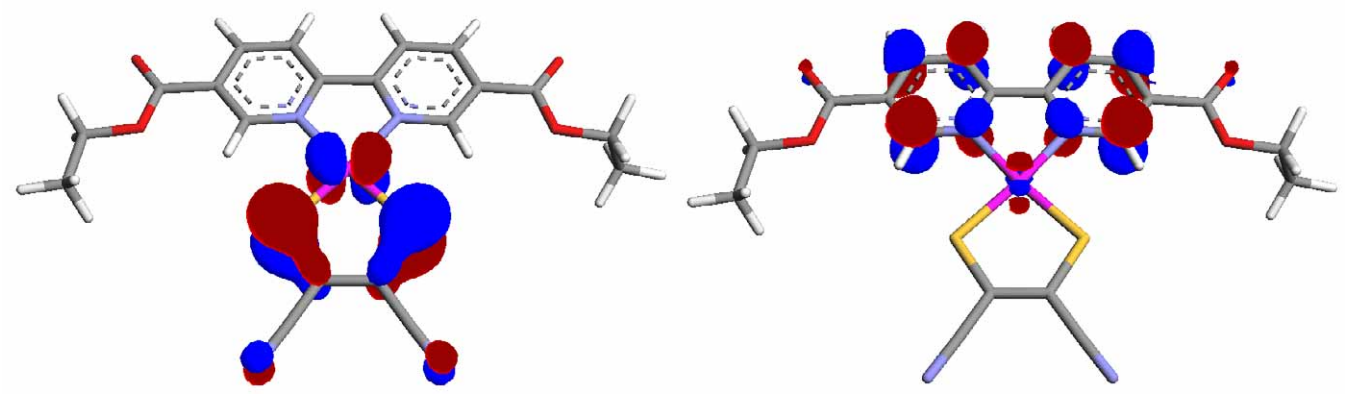

Fig. S15 Calculated HOMO-1 (left) and LUMO+1 (right) of **3c**

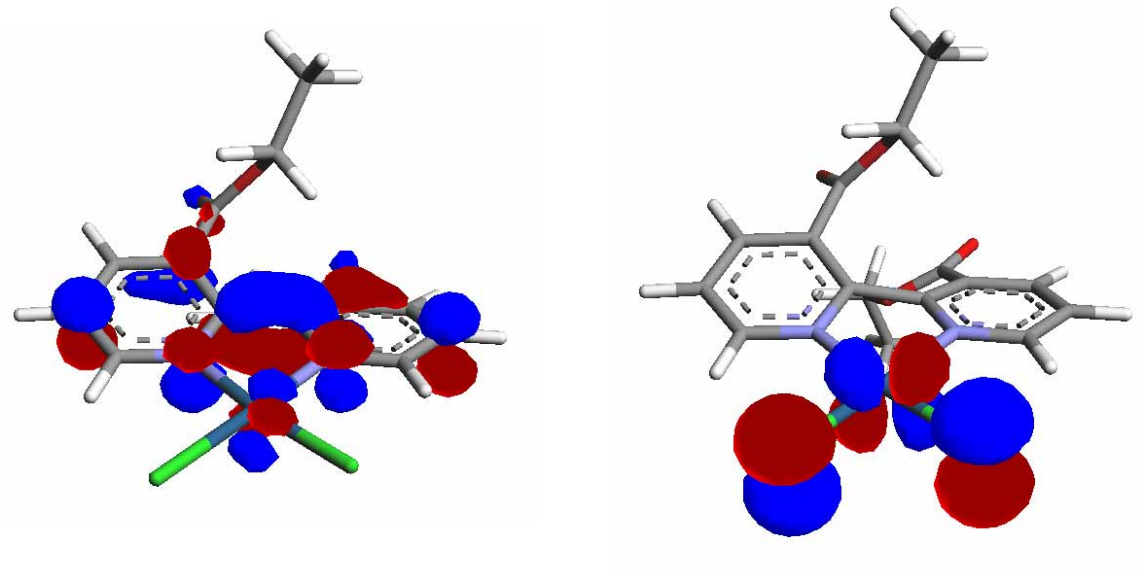

Fig. S16 Calculated LUMO (left) and HOMO of **1b** (right)

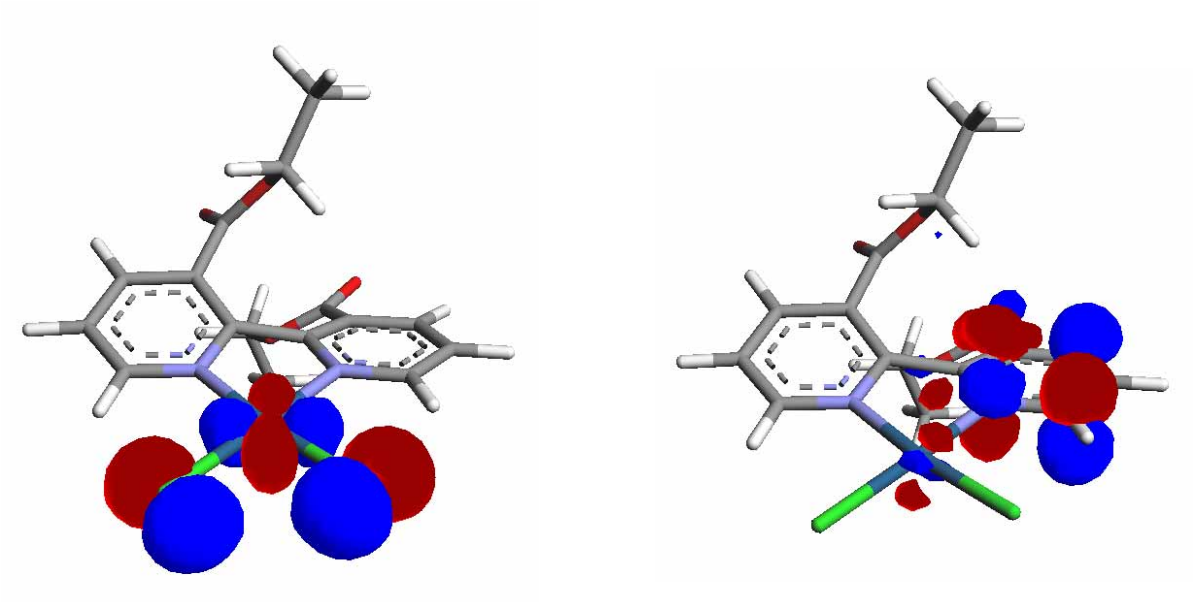

Fig. S17 Calculated HOMO-1 (left) and LUMO+1 (right) of **1b**

Atoms	Calculated Bond-length / Å	Angle / °	XRD Bond-length / Å	Angle / °
Pt(1)-N(2)	2.07466	-	2.058(8)	-
Pt(1)-N(3)	2.073106	-	2.074(10)	-
Pt(1)-S(21)	2.289272	-	2.245(3)	-
Pt(1)-S(14)	2.289536	-	2.258(2)	-
N(2)-Pt(1)-N(3)	-	78.29	-	79.4(3)
N(2)-Pt(1)-S(14)	-	96.87	-	96.2(2)
S(14)-Pt(1)-S(21)	-	88.32	-	89.54(9)
S(21)-Pt(1)-N(3)	-	96.93	-	95.3(1)
Torsion angle	-	28.13	-	30.7

Table S6 Comparison of calculated and XRD measured values of selected bond lengths and angles for **1c**

Complex	MO	Energies / eV	% Pt	% mnt	% bpy
1b	**HOMO**	-5.27194	42.93	-	4.78
	LUMO	-3.99001	7.84	-	88.16
1c	**HOMO**	-5.54187	11.76	79.06	9.2
	LUMO	-3.68551	5.77	6.89	87.33
2c	**HOMO**	-5.58922	10.62	79.04	10.33
	LUMO	-3.70973	8.32	7.5	84.17
3c	**HOMO**	-5.4801	11.13	79.11	9.76
	LUMO	-3.75272	5.22	6.56	88.21

Table S7 Calculated energies and % contributions of HOMO and LUMO for **1b**, **1c**, **2c**, and **3c**.

Complex	Excited State	Energy / cm^{-1} Calculated (nm)	Observed	*f*	Composition
1c	1	16180 (618)	18050 (554)	0.08	HOMO-LUMO 67 % (MMLL'CT) HOMO-LUMO+4 12 % (MMLL'CT)
	6	24940 (401)	26180 (382)	0.03	HOMO-LUMO+2 60% (MMLL'CT) HOMO-LUMO+4 31 % (MMLL'CT)
	7	26880 (372)		0.08	HOMO-2-LUMO 13 % (MLCT) HOMO-2-LUMO+4 10 % (MLCT) HOMO-LUMO+2 13 % (MMLL'CT) HOMO-LUMO+3 59 % (intraligand - mnt)
	12	32570 (307)	32260 (310)	0.2	HOMO-6-LUMO 15 % (intraligand – bpy) HOMO-4-LUMO 29 % (MMLL'CT) HOMO-3-LUMO 18 % (MLCT) HOMO-1-LUMO+1 54 % (MMLL'CT)
	18	34250 (292)		0.13	HOMO-2-LUMO+2 20 % (MLCT) HOMO-1-LUMO+2 15 % (MMLL'CT)

Table S8 TD-DFT results for **1c**. Only selected calculated transitions with relevant oscillator strengths have been included.

Complex	Excited State	Energy / cm^{-1} Calculated (nm)	Observed	*f*	Composition
2c	1	17450 (573)	18660 (536)	0.17	HOMO-LUMO 68 % (MMLL'CT)
	7	26600 (376)	27470 (364)	0.1	HOMO-2-LUMO+4 24 % (MLCT) HOMO-1-LUMO 10 % (MMLL'CT) HOMO-LUMO+2 59 % (LMCT)
	10	30960 (323)	31650 (316)	0.13	HOMO-4-LUMO 17 % (intraligand - bpy) HOMO-1-LUMO+1 67 % (MMLL'CT)
	13	32470 (308)		0.28	HOMO-4-LUMO 55 % (intraligand - bpy) HOMO-3-LUMO 12 % (MMLL'CT) HOMO-1-LUMO+1 15 % (MMLL'CT)
	15	33670 (297)		0.25	HOMO-5-LUMO 11 % (intraligand - bpy) HOMO-4-LUMO 10 % (intraligand - bpy) HOMO-3-LUMO 46 % (MMLL'CT) HOMO-1-LUMO+2 43 % (LMCT)

Table S9 TD-DFT results for **2c**. Only selected calculated transitions with oscillator strengths greater than 0.1 have been included.

Complex	Excited State	Energy / nm Calculated	Observed	*f*	Composition
3c	1	16450 (608)	18350 (545)	0.1	HOMO-LUMO 68 % (MMLL'CT)
	5	25640 (390)	25770 (388)	0.03	HOMO-LUMO+2 69 % (MMLL'CT)
	6	25710 (389)		0.04	HOMO-3-LUMO+1 10 % (MLCT) HOMO-2-LUMO+3 17 % (intraligand – mnt) HOMO-LUMO+1 61 % (intraligand – mnt)
	12	31950 (313)	31150 (321)	0.31	HOMO-3-LUMO 52 % (intraligand - bpy) HOMO-1-LUMO+2 42 % (MMLL'CT)
	15	33110 (302)	33900 (295)	0.2	HOMO-4-LUMO 16 % (MLCT) HOMO-2-LUMO+1 63 % (intraligand – mnt) HOMO-2-LUMO+4 16 % (MMLL'CT)
	18	33780 (296)		0.58	HOMO-3-LUMO 36 % (intraligand - bpy) HOMO-2-LUMO+2 17 % (MMLL'CT) HOMO-1-LUMO+2 53 % (MMLL'CT)

Table S10 TD-DFT results for **3c**. Selected calculated transitions with relevant oscillator strengths.

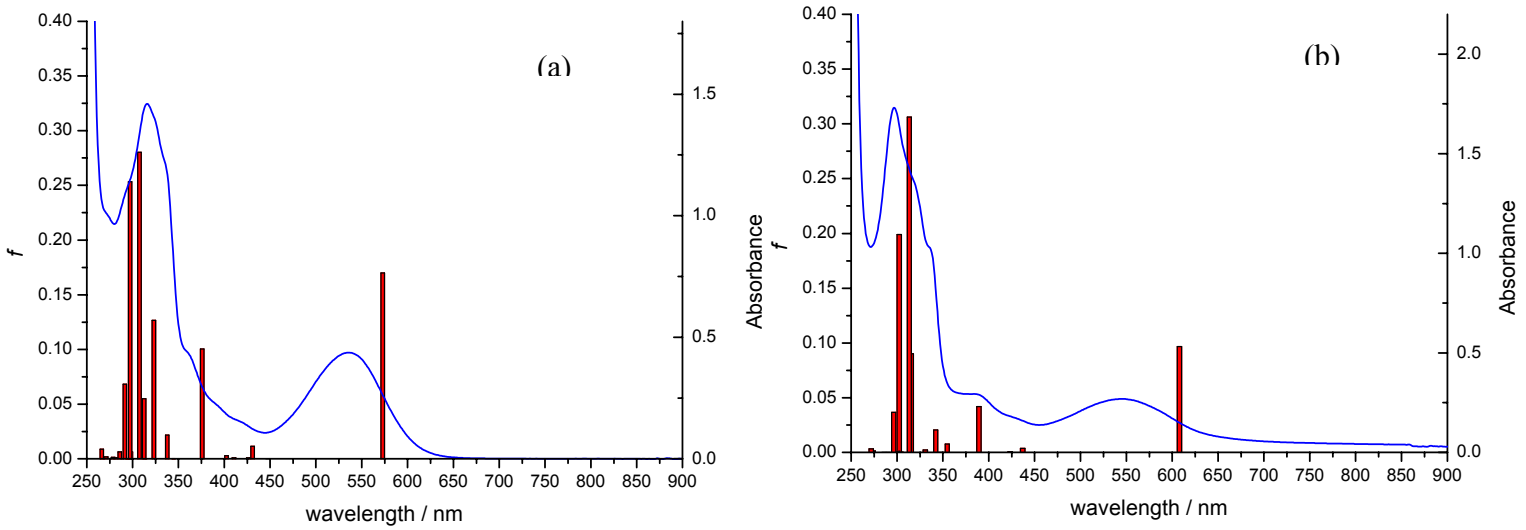

Fig S18 Calculated TD-DFT results (left axis) relative to the observed absorption spectrum (right axis) of a) **2c** and b) **3c.**